Proceedings of the
International Conference on Mechanical Engineering and Renewable Energy 2017
(ICMERE2017) 18 – 20 December, 2017, Chittagong, Bangladesh

ICMERE2017-PI-213

BOILING HEAT TRANSFER OF R134a FLOWING INSIDE A SMALL DIAMETER MICROFIN AND SMOOTH TUBE

M. Khairul Bashar[1], **Yuta Ichinose**[1], **A.R. Tuhin**[2], **Keishi Kariya**[3], **and Akio Miyara**[3]

[1]Graduate School of Science and Engineering, Saga University, 1 Honjo-machi, Saga,840-8502, Japan.
[2]Exchange student, Graduate School of Science and Engineering, Saga University, 1 Honjo-machi, Saga,840-8502, Japan and Student, Department of Mechanical Engineering, Chittagong University of Engineering & Technology, Bangladesh.
[3]Department of Mechanical Engineering, Saga University, 1 Honjo-machi, Saga, 840-8502, Japan.
khairul.me08@gmail.com*, 16575004@edu.cc.saga-u.ac.jp, metuhin12@gmail.com, kariya@me.saga-u.ac.jp and miyara@me.saga-u.ac.jp

Abstract*-The boiling heat transfer coefficient of the refrigerant R134a inside a microfin (D_h = 1.39 mm) and smooth (D_h =2.14 mm) horizontal mini tube was experimentally investigated. The experiment has been carried out under the conditions of mass flux varying from 50 to 200 (kg $m^{-2}s^{-1}$), the heat flux varying from 5 to 25 (kW m^{-2}), over the vapor quality range of 0.0 to 1.0. The saturation temperature at the inlet of the test section was kept constant and equal to 13ºC. The effect of mass flux, heat flux, vapor quality and tube geometry on heat transfer coefficients have been analyzed. The boiling heat transfer coefficient showed a mass flux and heat flux dependency. The experimental results also showed that the microfin tube heat transfer coefficient is higher than that of the smooth tube for all mass flux ranges. Experimental results have been compared with well-known correlations.*

Keywords: Boiling, Heat Transfer Coefficient, Two-Phase Flow, Microfin tube, Smooth tube

1. INTRODUCTION

Nowadays, microfin and smooth mini tube are present in many applications ranging from different heat exchangers in the process industry to automotive, HVAC and domestic applications. Especially, since the invention of microfin tubes has received a lot of attention because they can assure higher heat transfer coefficients compared to smooth tubes, with a relatively small increase of pressure drop, Fujie et al. [1]. Microfin tubes with internal diameters smaller than 3 mm are becoming more and more popular because they can be used in the next generation air conditioning and refrigeration system, leading to more compact and more efficient heat exchangers. In addition, the use of these mini microfin tubes may imply a large reduction of the refrigerant charge of the system, thus facing with the new stricter environmental regulations. For these reasons, researchers have a strong interest in understanding the heat transfer characteristics of microfin mini tube.

Boiling heat transfer has been studied extensively for many years, but the open literature about small diameter smooth and microfin tubes (i.e. inner diameter lower than 2.5 mm) is poor if compared with larger tubes. Choi et al. [2] carried out an experimental study on boiling heat transfer of R22, R134a and CO_2 in a horizontal smooth tube, having an inner diameter of 1.5 mm and 3.0 mm. The mass and heat fluxes ranged from 200-600 (kgm^{-2}s^{-1}) and 10-40 (kW m^{-2}) respectively at a saturation temperature of 10^{o}C. Heat transfer coefficients were also compared to those of R22, R134a and CO_2. The heat transfer results show heat flux and mass flux dependency. Saitoh et al. [3] experimentally studied the boiling heat transfer mechanism of R134a in tubes with inner diameter of 0.51, 1.12, and 3.1 mm; the authors studied the effect of tube diameter and finally modified the Chen-type correlation.

Kondou et al. [4] studied the flow boiling of R32, R1234ze(E), and R32/R1234ze(E) mixtures in a horizontal microfin tube with an inner diameter of 5.2 mm. Experiments were run at a saturation temperature of 10^{o}C, heat fluxes of 10 and 15 (kW m^{-2}), and mass fluxes from 150-400 (kg m^{-2}s^{-1}). Results showed that, the mixture has a lower heat transfer coefficient than both pure refrigerants. They also propose a new correlation. Daini et al. [5] experimentally studied the flow boiling of R1234ze(E) inside a microfin tube with an internal diameter at the fin tip of 3.4 mm. They studied the effect of vapor quality, mass flux, and heat flux on the heat transfer coefficient, pressure drop, and vapor quality at the onset of the dryout phenomena. Furthermore, the authors proposed two correlations to estimate the heat transfer coefficient in the region pre-dryout and the frictional pressure. Wu et al. [6] performed flow boiling experiments of R22 and R410A inside smooth and microfin tubes.

2. EXPERIMENTAL APPARATUS AND PROCEDURE

Figure 1 shows the schematic diagram of the experimental apparatus used in this study. The experimental test facility consists of a test section, refrigerant loop, cooling/heating water loop, sub-cooling loop and data acquisition system. The liquid refrigerant is pumped by an independently controlled gear pump magnetically coupled to a variable speed electric motor through, a filter, mixer, pre-heaters, sight glass tube, test section cooler and accumulator. The quality of refrigerant before entering the test section is controlled by first pre-heater. The sub-cooled refrigerant then enters the test section to get experimental data in the vapor quality range of 0.1 to 0.9. Three mixing chambers are installed at the inlet of first pre-heater and the test section and outlet of the test section to measure the bulk temperature of the refrigerant. The system pressure of the test apparatus is controlled by the accumulator. The absolute pressure transducer, differential pressure transducer and K-type thermocouple at various positions and sight glass at the inlet and outlet of the test section are installed as shown in Fig. 1 to monitor the refrigerant's state. All of the signals from the pressure transducer and thermocouples are collected by a data acquisition system. The whole test apparatus is well insulated with special attention given to the test section.

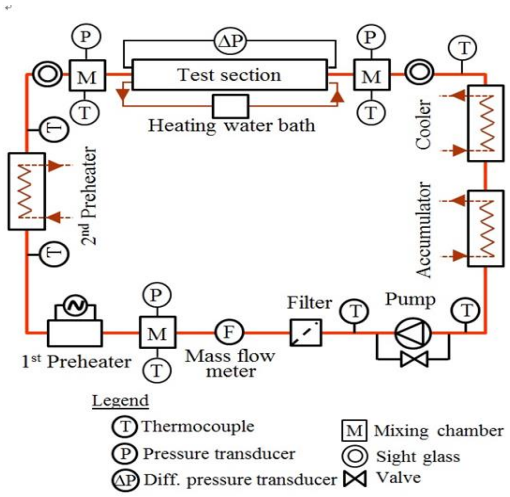

Fig.1: Schematic diagram of experimental apparatus

Figure 2 shows the schematic diagram of the test section for the present study. The test section consists of a horizontally installed copper tube, two headers and three cooling water channels. The test tube is a small diameter microfin tube with an outer and equivalent diameter of 2.5 and 2.15 mm respectively. The parameters of the microfin test tube are as follows: number of fins - 25, helix angle - 31°, fin height - 0.1 mm. The outer and equivalent diameter of a smooth tube is 2.5 and 2.14 mm respectively. The cooling water channels are designed as a tube in tube heat exchanger and used to supply heat flux to the tested tubes. The total length of each test section is 852 mm and the effective cooling length is 744 mm. A differential pressure transducer with a calibrated accuracy of ±0.001 (MPa) is installed in the header to measure the pressure difference. The inlet and outlet refrigerant temperature are measured by two K-type thermocouples with calibrated accuracy of ± 0.03 ^{o} C installed in the inlet and outlet mixing chambers. The inlet and outlet pressure are measured by two pressure transducer with calibrated accuracy of ± 0.001 (MPa) inserted in the inlet and outlet mixing chambers. For measuring the inlet and outlet cooling water temperatures, K-type thermocouples with calibrated accuracy of ±0.03 ^{o}C are also installed at the inlet and outlet of each subsection. The heat balance factors of the most test runs are under ± 10% as shown in Fig. 3. The experiment was conducted over the mass and heat flux range from 50 to 200 (kg m^{-2}s^{-1}) and 7 to 30 (kW m^{-2}) respectively, vapor quality ranges from 0.1 to 0.98 and saturation temperature is 13^{o}C. The thermodynamic properties of R134a were obtained from REFPROP 9.1 [7].

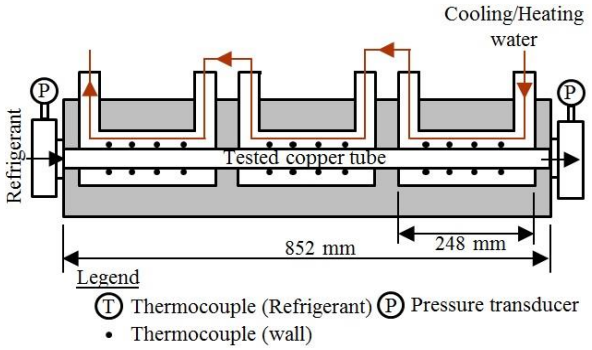

Fig. 2: Schematic view of the test section

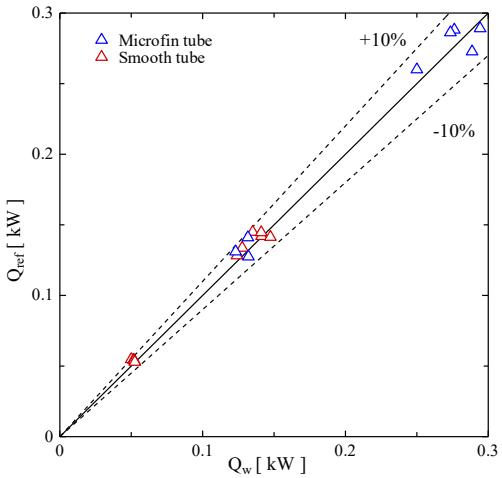

Fig.3: Error in heat balance measurement of all the test runs

3. DATA REDUCTION

The local heat transfer coefficient of each subsection during the boiling was calculated by Eq. (1)

$$\mathrm{HTC} = \frac{q}{T_{wi} - T_b} \qquad (1)$$

Where, HTC is the heat transfer coefficient, q is the

heat flux, T_{wi} is the inner wall temperature and T_b is the bulk temperature that is the equilibrium saturation temperature.

In this present experiment, the inner wall temperature is calculated from the measured outer wall temperature with one-dimensional heat conduction equation. Therefore, the heat flux of each subsection is calculated by Eq. (2).

$$q = \frac{Q_w\, HB}{\pi d_i\, \Delta Z} \tag{2}$$

The heat balance factor is calculated by Eq. (3)

$$\mathrm{HB} = \frac{Q_{ref}}{Q_w} \tag{3}$$

The heat gain of refrigerant from inlet to the exit of the whole test section is calculated by Eq. (4)

$$Q_{ref} = W_{ref}(h_{ref,O} - h_{ref,I}) \tag{4}$$

Inlet enthalpy and $h_{ref,O}$ of the whole test section are obtained from the REFPROP 9.1 [7] at a measured refrigerant temperature and pressure of the corresponding point. The heat release of the water from the inlet to the exit of the whole test section is calculated by Eq. (5).

$$Q_w = W_w C_{p,s}(T_{wO} - T_{wI}) \tag{5}$$

The vapor quality in the test section is calculated by the following Eq. (6).

$$x = \frac{h_x - h_l}{h_v - h_l} \tag{6}$$

All experimental data were collected after the steady state was reached for temperature, pressure, and refrigerant flow.

4. RESULTS AND DISCUSSION

4.1 Experimental Results

Experimental data points of R134a are plotted on the Wojtan et al. [8] flow pattern map where the data covers for mass fluxes range of 50-200 (kg $m^{-2}s^{-1}$) and vapor quality range of 0.0-1.0, as shown in Fig.4. The flow pattern map has been drawn for saturation temperature of 13 °C. The transition lines of dryout is calculated for experimentally obtained heat fluxes of 13 (kW m^{-2}), 13 (kW m^{-2}) and 25 (kW m^{-2}) of 50 (kg $m^{-2}s^{-1}$), 100 (kg $m^{-2}s^{-1}$) and 200 (kg $m^{-2}s^{-1}$) respectively. It is seen from this flow pattern map that there is a minor variation among the transitional vapor quality (X_{IA}) between the intermittent flow and annular flow of 50, 100 and 200 (kg $m^{-2}s^{-1}$), because (X_{IA}) is a function of density and viscosity ratio. However, at mass flux G= 200 (kg $m^{-2}s^{-1}$), almost all the data points are lapped in intermittent and annular flow regime. Dry out is also found at high qualities region for mass flux 100 and 200 (kg $m^{-2}s^{-1}$), although dry out is not found for mass fluxes G=50 (kg $m^{-2}s^{-1}$). At G=50 and 100 (kg $m^{-2}s^{-1}$), some data points are lapped in slag and stratified wavy flow regime.

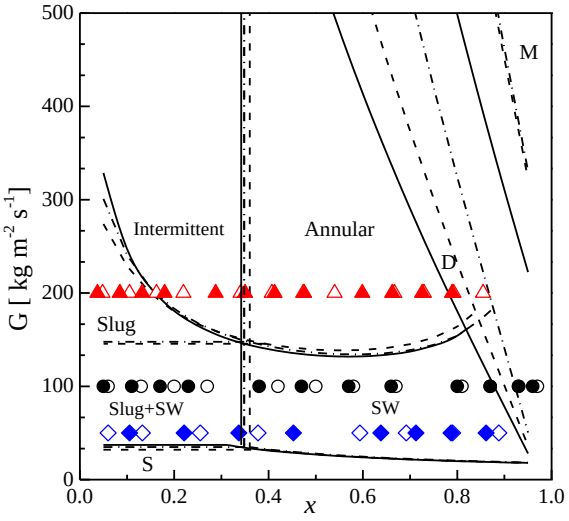

Fig.4: Experimental Boiling data overlaid on the Wojtan et al. [8] flow pattern map.

Figure 5 shows the experimental result of heat transfer coefficient as a function of vapor quality at heat flux 12 (kW m^{-2}) and saturation temperature of 13ºC. The Fig. 5 (a) shows the effect of mass flux in smooth tube and Fig. 5 (b) shows the effect of mass flux in microfin tube. From both these figures, it is seen that, at the low mass flux of 50 (kg $m^{-2}s^{-1}$), the heat transfer coefficient slightly increased with vapor quality and no dryout occur. On the contrary, at the mass flux of 100 (kg $m^{-2}s^{-1}$), the heat transfer coefficient remains almost constant for both tubes at a value of q = 12 (kWm^{-2}), up to a vapor quality of approximately 0.3, and then it increases with vapor quality, it reaches a maximum value and then suddenly decrease because of dryout phenomena. The maximum heat transfer coefficient is shown in vapor quality of 0.57 for microfin tube and the dryout quality is about 0.8 as shown in Fig. 5 (b).

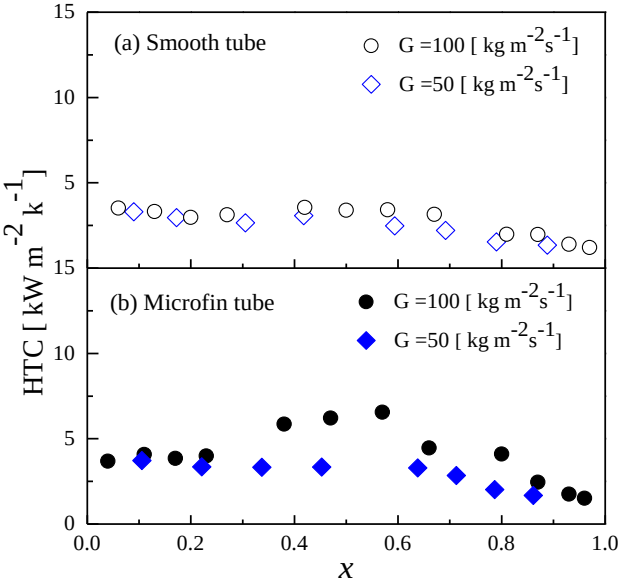

Fig.5: Effect of mass fluxes and vapor quality on boiling heat transfer coefficient at T_{sat}=13 °C (a) Smooth tube (b) Microfin tube.

Figure 6 shows the comparison of experimental and predicted heat transfer coefficient of G= 200 (kg $m^{-2}s^{-1}$) at heat flux 25 (kW m^{-2}) by Takamatsu et al. [9]. The dash line represents the force convection (α_{cv}) heat transfer component, estimated by the correlation of Takamatsu et al. [9]. The solid line represents the prediction of the total heat transfer coefficient (α_{pre}), calculated by the same correlation. The difference between predicted heat transfer coefficient and force convection component denotes the nucleate boiling component (α_{nb}). However, this graph trend can be explained considering the two competitive mechanisms that control the boiling phenomena: nucleate boiling and forced convection. For the smooth tube at low vapor qualities, nucleate boiling seems to be the controlling phenomenon, and no effect of vapor quality on the heat transfer coefficient is visible up to quality 0.3, when the vapor quality exceeds 0.4, the heat transfer coefficient increases with increasing vapor quality. Therefore, at high-quality region forced convection plays a more important role in the phase change mechanism. Furthermore, nucleate boiling component, α_{nb} is decreased in a noticeable degree for both tube and heat transfer coefficient is dominant by forced convection. The similar experimental result is also reported by Diani et al. [10].

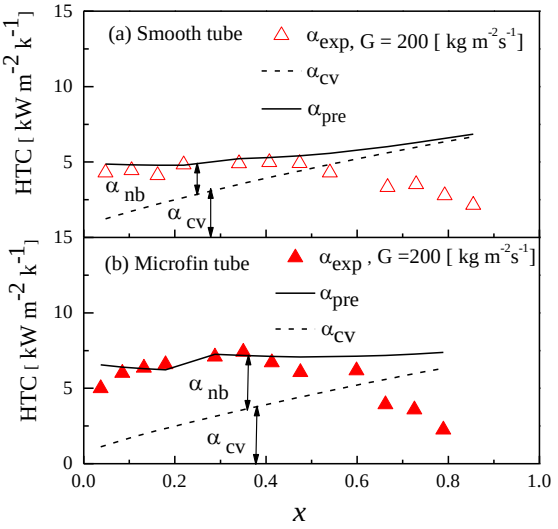

Fig.6: Comparison of experimental and predicted heat transfer coefficient for G= 200 [kgm^{-2}s^{-1}] at T_{sat}=13ºC by Takamatsu et al. [9] (a) Smooth tube (b) Microfin tube.

Figure 7 shows the effect of heat flux on the heat transfer coefficient and this Fig.7 plotted as the heat transfer coefficient against the vapor quality. The Fig. 7 (a) is for smooth tube, in this case mass flux was kept at 50 (kgm^{-2}s^{-1}) and compared the measured results for two different heat fluxes: 7 and 13 (kWm^{-2}). Increasing the heat flux from 7 to 13 (kWm^{-2}) shows that the heat transfer coefficient increases with heat flux up to quality o.8. The Fig.7(b) is for the microfin tube, mass flux was kept at 200 (kg $m^{-2}s^{-1}$) and compared the measured results for two different heat fluxes: 25 and 30 (kW m^{-2}). Increasing the heat flux from 25 to 30 (kW m^{-2}) showed the heat transfer coefficient is almost same at low quality region and then it increases with quality. Thus, in this case, force convection boiling effect is more dominant than nucleate boiling.

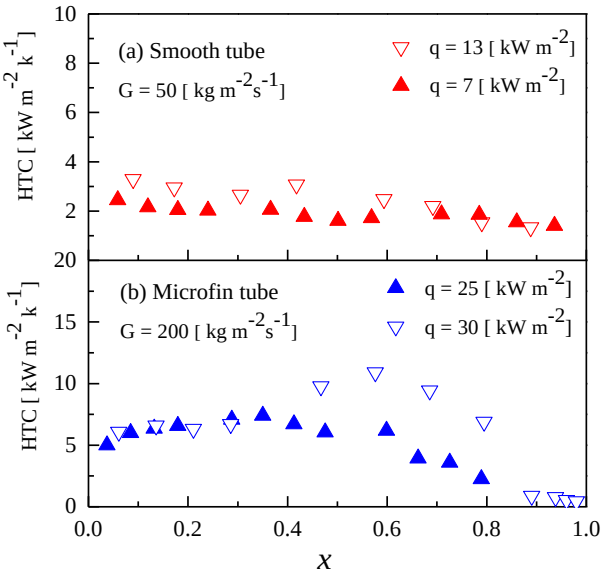

Fig.7: Effect of heat flux on heat transfer coefficient at T_{sat} =13ºC (a) Smooth tube (b) Microfin tube.

4.2 Comparison with correlations

The experimental data were compared against existing correlations to predict the boiling heat transfer coefficient. Two boiling heat transfer correlations were proposed by Choi et al. [2] and Saitoh et al. [3] as shown in Table 1.

Table 1: Correlation from literature

Author (s)	Correlation
Choi et al. [2]	$\alpha_{tp} = E\alpha_1 + S\alpha_{SA}$, $\alpha_1 = 0.023 Re_l^{0.8} Pr_l^{0.4} \frac{\lambda_1}{d_i}$, $\alpha_{SA} = 207 \frac{\lambda_1}{d_b}\left(\frac{q d_b}{\lambda_1 T_{sat}}\right)^{0.674}\left(\frac{\rho_v}{\rho_l}\right)^{0.581} Pr_l^{0.533}$, $d_b = 0.0146\beta x[2\sigma/(g(\rho_1-\rho_v))]^{0.5}$, $E = c_1 Bo^{c2} X_{tt}^{c3}, S = c_4 Co^{c5}$ Experimental conditions: R32, R134a, d_i=7.75 mm, G = 240-1060 (kg $m^{-2}s^{-1}$)
Saitoh et al. [3]	$\alpha_{tp,pre} = F\alpha_1 + S\alpha_{pool}$, $S = \left(1 + \alpha\left(Re_{tp} \times 10^{-4}\right)^n\right)^{-1}$, $F = 1 + \frac{\left(\frac{1}{X_{tt}}\right)^2}{1+We_v^m}$, $We_v = G^2 d_i/(\sigma\rho_V)$, $Re_{tp} = Re_l F^{1.25}$, $\alpha_{pool} = 207 \frac{\lambda_1}{d_b}\left(\frac{q d_b}{\lambda_1 T_{sat}}\right)^{0.745}\left(\frac{\rho_v}{\rho_l}\right)^{0.581} Pr_l^{0.533}$ Experimental conditions: d_i= 0.5-11 mm Refrigerant: R134a

The first comparison, depicted in Fig. 8(a), shows the experimental data was predicted by Choi et al. [2]. This correlation was developed for a 7.75 mm horizontal smooth tube. This correlation also predicts the experimental data fairly well with a MD = 26.740 % and AD = 26.740 %. Especially, about 90 % of the smooth tube data were predicted within ±30%.

A chen-type correlation for flow boiling heat transfer of R134a in a horizontal tube was modified talking into account the effect of tube diameter by Saitoh et al. [3]. However, this correlation captured the majority of the experimental data points; AD and MD are 10.910 %, 32.912% respectively as shows in Fig. 8(b).

(a)

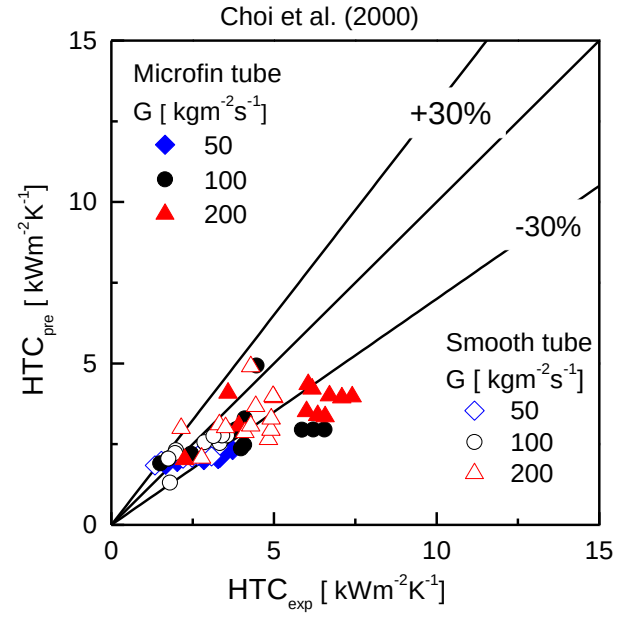

(b)

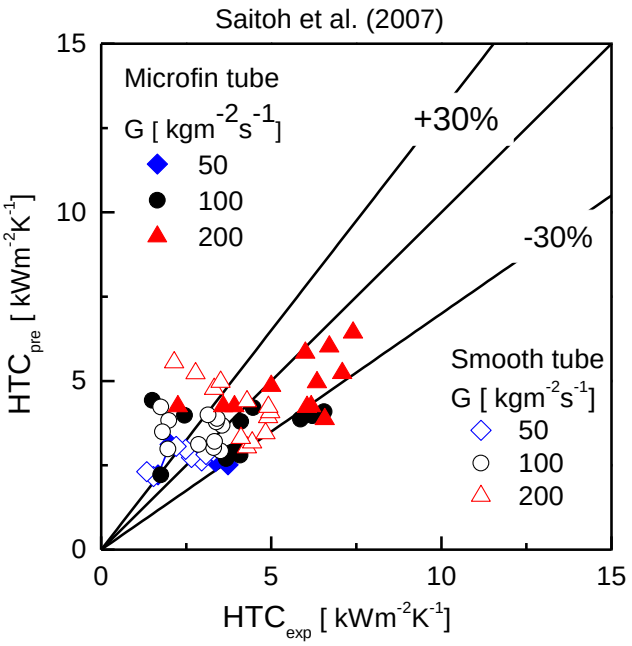

Fig. 8: Comparison of experimental average heat transfer coefficient with (a) Choi et al. [2] (b) Saitoh et al. [3]

5. CONCLUSION

The boiling heat transfer coefficient of R134a has been measured experimentally and compared with two correlations. The Wojtan's flow pattern map is drawn and analyzed the experimental data. The average heat transfer coefficients were measured at mass fluxes of 50-200 (kg $m^{-2}s^{-1}$), heat fluxes of 7-30 (kWm^{-2}), and saturation temperature of 13ºC. The results are summarized as follows.

(1) The boiling heat transfer coefficient of the microfin tube is about 1.32-1.85 times higher than the smooth tube.

(2) The boiling results show that the phase change mechanism is controlled by the nucleate boiling and two-phase forced convection. At low vapor quality (x<0.4), nucleate boiling heat transfer is the dominant heat transfer mechanism, and at high vapor quality, forced convective boiling is dominant.

(3) In the low-quality region for G= 50 (kg $m^{-2}s^{-1}$), it is observed a noteworthy influence of heat flux on the heat transfer coefficient while, in the high vapor quality region this tended to vanish, and the coefficient decreased. On the contrary, for G= 200 (kg $m^{-2}s^{-1}$), increasing the heat flux this trend is opposite because of more forced convection boiling effect.

(4) The prediction performance of the correlations is calculated by mean deviations (MD). The prediction performance of the correlations in ascending order is Saitoh et al. → Choi et al.

6. ACKNOWLEDGEMENT

The authors would like to thank the Japan Copper Development Association for their kind support.

7. REFERENCES

[1] K. Fujie, N. Itoh, H. Kimura, N. Nakayama, T. Yanugi, "Heat transfer pipe", US Patent 4044797, Assigned to Hitachi, 1977.

[2] K. Choi, A.S. Pamitran, Y.O. Chun, T. O. Jong, "Evaporation heat transfer of R32, R134a, R32/R134a, and R32/125/134a inside a horizontal smooth tube", International Journal of Refrigeration, Vol. 43, pp. 3651-3660, 2000.

[3] S. Saitoh, H. Daiguji, E. Hihara, "Correlation for boiling heat transfer of R-134a in horizontal tubes including effect of tube diameter", International Journal of Heat and Mass Transfer, Vol. 50, pp. 5215-5225, 2007.

[4] C. Kondou, D. Baba, F. Mishima, S. Koyama, "Flow boiling of non-a zeotropic mixtures R32/R1234ze(E) in horizontal microfin tubes", International Journal of Refrigeration, Vol. 36, pp. 2366-2378, 2013.

[5] A. Daini, S. Mancin, L. Rossetto, "R1234ze(E) flow boiling inside a 3.4 mm ID microfin tube", International Journal of Refrigeration, Vol. 47, pp. 105-119, 2014.

[6] Z. Wu, Y. Wu, B. Sunden, W. Li, "Convective vaporization in micro-fin tubes of different geometries", Experimental Thermal and Fluid

Science, Vol. 44, pp. 398-408, 2013.
[7] E.W. Lemmon, M.L. Huber, M.O. McLinden, "Reference Fluid Thermodynamic and Transport Properties-REFPROP", Version 9.1, NIST Standard Reference Database 23, Gaithersburg, 2013.
[8] L. Wojtan, T.Ursenbacher, J.R.Thome, "Investigation of flow boiling in horizontal tubes: part I-A new adiabatic two-phase flow pattern map", International Journal of heat and mass transfer, Vol. 48, pp. 2955-2969, 2005.
[9] H. Takamatsu, S. Momoki, T. Fuji, "A correlation for forced convective boiling heat transfer of pure refrigerants in a horizontal smooth tube", International Journal of Heat and Mass Transfer, Vol. 36, pp. 3351-3360, 1993.
[10] A. Diani, S. Mancin, L. Rossetto, "Flow boiling heat transfer of R1234yf inside a 3.4 mm ID micro-fin tube", Experimental Thermal and Fluid science, Vol. 66, pp.127-136, 2015.

8. NOMENCLATURE

Symbol	Meaning	Unit
AD	Average deviation	Dimensionless
Bo	Bond number	Dimensionless
b	Fin root distance	(m)
C_o	Convection number	Dimensionless
C_p	Isobaric specific heat	(kJ $kg^{-1}K^{-1}$)
C_v	Forced convection	Dimensionless
d	Diameter	(mm)
D_h	Hydraulic diameter	(mm)
F	Heat transfer enhancement factor	Dimensionless
G	Mass flux	(kg $m^{-2}s^{-1}$)
g	Gravitational acceleration	(m s^{-2})
h	Enthalpy	(kJ kg^{-1})
HTC	Heat transfer coefficient	(kW m^{-2} K^{-1})
MD	Mean deviation	Dimensionless
n_b	Nucleate boiling	Dimensionless
Pr	Prandtl number	Dimensionless
q	Heat flux	(kW m^{-2})
Re_l	Liquid Reynolds number	Dimensionless
T	Temperature	(ºC)
w	Mass flow rate	(kg s^{-1})
x	Quality	Dimensionless
X_{tt}	Lockhart martinelli parameter	Dimensionless
$\triangle Z$	Length of sub-section	(m)
Greek symbols		
α	Heat transfer coefficient	(kW $m^{-2}K^{-1}$)
β	Helix angle of fin	(º)
λ	Thermal conductivity	(kW $m^{-1}k^{-1}$)
ρ	Density	(kg m^{-3})
σ	Liquid film thickness	(m)

Subscripts		
b	Bulk	Dimensionless
E	Enhancement factor	Dimensionless
HB	Heat balance	Dimensionless
i	Inner	Dimensionless
I	Inlet	Dimensionless
L/l	Liquid	Dimensionless
o	Outlet	Dimensionless
Pre	Predicted	Dimensionless
ref	Refrigerant	Dimensionless
S	Suppression factor	Dimensionless
s	Heat source water	Dimensionless
Sat	Saturation	Dimensionless
tp	Two-phase	Dimensionless
v	Vapor	Dimensionless
w	Water	Dimensionless
Wi	Inner wall	Dimensionless